



# Regularization Approach for Network Modeling of German Energy Market

Shi Chen \*

Wolfgang Karl Härdle \*<sup>2</sup>

Brenda López Cabrera \*<sup>2</sup>



\* Karlsruher Institut für Technologie, Germany

\*<sup>2</sup> Humboldt-Universität zu Berlin, Germany

This research was supported by the Deutsche  
Forschungsgemeinschaft through the  
International Research Training Group 1792  
"High Dimensional Nonstationary Time Series".

<http://irtg1792.hu-berlin.de>  
ISSN 2568-5619

# Regularization Approach for Network Modeling of German Energy Market \*

Shi Chen <sup>†</sup>, Wolfgang Karl Härdle<sup>‡</sup>, Brenda López Cabrera <sup>§</sup>

We investigate the concept of connectedness, which is important for risk measurement and management in German energy market. Understanding and learning from these mechanisms are essential to avoid future systemic disasters. To deal with large portfolio selection, we propose regularization approach to capture the spillover and contagion effects across German power derivatives. This paper shows how network analysis can facilitate the monitoring of futures price movements. Our methodology combines high-dimensional variable selection techniques with network analysis, the results show that contracts like Phelix Base Year Options and Phelix Peak Year Futures are in the core of the Energy futures market.

**Keywords:** regularization, energy risk transmission, network, German energy market

**JEL:** C1, Q41, Q47

---

\*The financial support from the Deutsche Forschungsgemeinschaft via SFB 649 "Ökonomisches Risiko", Humboldt-Universität zu Berlin and IRTG 1972 "High Dimensional Non Stationary Time Series" is gratefully acknowledged.

<sup>†</sup>Corresponding author, Chair of Statistics and Econometrics, Karlsruher Institut für Technologie, Blücherstr.17, 76185 Karlsruhe, Germany. Email: shi.chen@kit.edu

<sup>‡</sup>School of Business and Economics, Humboldt-Universität zu Berlin, Unter den Linden 6, 10099 Berlin, Germany; Singapore Management University, 50 Stamford Road, Singapore 178899

<sup>§</sup>School of Business and Economics, Humboldt-Universität zu Berlin, Unter den Linden 6, 10099 Berlin, Germany

# 1 INTRODUCTION

Affordable and reliable energy supply is essential for industrial growth. Achieving these in times of growing demand, raw materials shortage and climate change poses challenges. It is therefore essential to provide precise forecast for future power supply. Germany's power system for the industry and the consumers is undergoing radical change. At present, conventional energy sources generate approximately 74% of Germany's electricity. However, the ongoing expansion of renewable energy and the phase-out of nuclear energy for power generation will change the composition of the electricity mix, which in return, will generate pricing signals affecting the electricity trading. Therefore a study on the electricity derivative market, e.g. the forward market can provide a hedge against such risks. Based on such insights, energy companies may invest in both electricity spot and derivatives markets. However, the number of variables and relevant factors is typically huge. A properly designed subset selection must be employed to pick the most informative power contracts to representing energy market risk.

High-dimensional statistical problems arise from diverse fields of scientific research and technological development, including energy markets. The traditional idea of best subset selection methods is computationally too expensive for many modern statistical applications. Variable selection techniques have therefore been successfully developed in recent years and they indeed play a pivotal role in contemporary statistical learning and techniques. Researchers have proposed various penalized estimators, a preminent example being the least absolute selection and shrinkage operator (lasso) of Tibshirani (1996). In recent years, lasso has been extended to high-dimensional cases, see Bickel et al. (2009). Other popular methods contribute to the literature, such as smoothly clipped absolute deviation (SCAD) Fan and Li (2001), adaptive Lasso of Zou (2006), elastic net estimator of Zou and Hastie (2005), Dantzig selector of Candès and Tao (2007). In an ultra high-dimensional case where the dimensionality of the model is allowed to grow exponentially in the sample size, it is helpful to begin with screening to delete some significantly irrelevant variables

from the model. Fan and Lv (2008) introduce a method called sure independence screening (SIS hence-after) for this goal. Even when the regularity conditions may not hold, Fan et al. (2009) extend the iterated-SIS method to work by iteratively performing feature selection to recruit a small number of features.

The German power market is highly interconnected with a dense and wide range of electricity derivative contracts. In this paper we investigate the concept of connectedness, which is important for risk measurement and management. We aim to build up a sparse network in which nodes represent power contracts and links represent the magnitude of connectedness, local shocks and events can therefore be easily amplified and turned into global events. Understanding and learning from these mechanisms are essential to avoid future systemic disasters. Regularization approach is needed to capture significant spillover and contagion effects in the energy market. To better understand the interaction between power contracts, the iterated-SIS method combined with penalized estimators are applied to estimate the sparse web of connections. Our network of interest is constructed in the context of time series based on vector autoregression (VAR) models, the iterated-SIS methods are of much use when building VAR models since the number of parameters to estimate increases quadratically in the number of variables included. In addition, asymptotic properties of lasso for high-dimensional time series have been considered by Loh and Wainwright (2011), Wu et al. (2016). Kock and Callot (2015) establish the high-dimensional VAR estimation with focus on lasso and adaptive lasso. Basu et al. (2015) investigate the theoretical properties of regularized estimates in sparse high-dimensional time series models when the data are generated from a multivariate stationary Gaussian process.

To quantify the associations between individual power contract and energy exchange market, the network we constructed is obtained from the forecast error variance decomposition (FEVD) based on VAR estimates in the framework of Koop et al. (1996) and Pesaran and Shin (1998). This kind of connectedness measure is also used by Diebold and Yilmaz (2014) for conceptualizing and empirically measuring weighted, directed networks at a variety

of levels. Related is Demirer et al. (2017) who use lasso method to select, shrink and estimate a high-dimensional network. Related empirical work are with more focus on financial banking contexts, for examples see Acharya et al. (2012), Hautsch et al. (2014), Giglio et al. (2016), Babus (2016), Brownlees and Engle (2016), Acharya et al. (2017). There is, however, no research on energy connectedness. This is particularly unfortunate given the role of the liberalization of the energy market and the inclusion of renewables. While estimates of the network yield the qualitative links between power contracts, individual impact from specific contract can be estimate and speculate accordingly. Hence the risk contribution from the market component can be identified clearly, this will help us to learn more about the German power market functioning and environment. For example, the results show that day-ahead spot power contracts that bidding between 9am and 13am are in the core of the energy futures market, the key derivatives in connecting markets can be identified.

The rest of the paper proceeds as follows. Section 2 summarizes the energy market. In section 3, we describe in details how the regularization approach is applied to estimate the large portfolio and how the network is constructed. Section 4 presents the empirical results by starting with a discussion of variable selection. Finally section 5 concludes.

## 2 OVERVIEW OF ENERGY MARKET

### 2.1 GERMAN ELECTRICITY DERIVATIVE MARKET

The German electricity market is Europe's largest, with annual power consumption of around 530 TWh and a generation capacity of 184 GW. As a net energy exporter, the export capacity of Germany is expected to continue to grow as planned interconnections expand cross-border transmission capacity with several neighboring countries. Germany has significant interconnection capacity with neighboring EU member states as well. It is interconnected with Austria, Switzerland, the Czech Republic, Denmark, France, Luxembourg, the Netherlands, Poland, and Sweden. To maintain stable and reliable supply of electricity, the so-

called Transmission system operators (TSOs) keep control power available. Primary control, secondary control, and tertiary control reserve are procured by the respective TSOs within a non-discriminatory control power market in accordance with the requirements of the Federal Cartel Office. Demand for control energy is created when the sum of power generated varies from the actual load caused by unforeseeable weather fluctuations in the case of renewable energies.

Electricity is traded on the exchange and over the counter. Standardized products are bought and sold in a transparent process on the exchange, which, for Germany, is the European Energy Exchange EEX in Leipzig, the European Energy Exchange EPEX SPOT in Paris and the Energy Exchange Austria (EXAA) in Vienna. The European Energy Exchange (EEX) is the leading energy exchange in Europe. It develops, operates and connects secure, liquid and transparent markets for energy and commodity products. Contracts on power, coal and CO<sub>2</sub> emission allowances as well as freight and agricultural products are traded or registered for clearing on EEX. EPEX SPOT, Powernext, Cleartrade Exchange (CLTX) and Gaspoint Nordic are also members of EEX Group. The German wholesale electricity market is broadly made up of three elements, a forward market, a day-ahead market and an intra-day market. These submarkets generate the pricing signal which electricity production and consumption align to. The objective of this paper is to analyse the interaction of different future contracts traded in the forward market, whether forward market is influenced by market power of spot prices traded in EPEX market.

Electricity providers and electricity purchasers submit their bids in their national day-ahead market zones. The exchange price on the day-ahead market is determined jointly for coupled markets. Electricity providers and electricity purchasers submit their bids in their national day-ahead market zones. In an iterative process, the demand for electricity in the market zone is served by the lowest price offers of electricity from all the market areas until the capacity of the connections between the market zones (cross-border inter-connectors) is fully utilized. As long as the cross-border inter-connectors have sufficient capacity, this

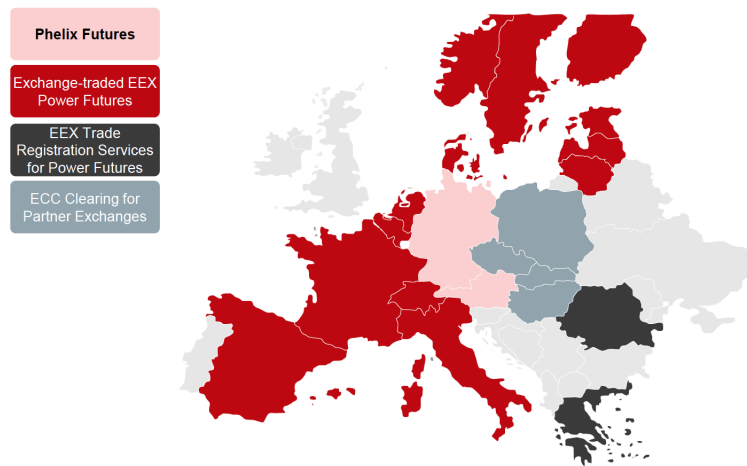


Figure 2.1: The distribution of European power derivatives in EEX market. Source: EEX website

process aligns the prices in the coupled market areas. On account of market coupling, the national power demand is covered by the international offers with lowest prices. The upshot is that on the whole less capacity is required to meet the demand. As shown in Figure 2.1, Phelix Future, as the product traded in Germany, is a financial derivatives contract settling against the average power spot market prices of future delivery periods for the German/Austrian market area.

## 2.2 PHELIX FUTURES

Electricity supply deliveries in the forward market can be negotiated up to seven years in advance, but for liquidity reasons typically only look out three years, and in fact one year ahead futures are traded at most. The Phelix Future is a financial derivatives contract referring to the average power spot market prices of future delivery periods of the German/Austrian market area.

As the most liquid contract and benchmark for European power trading, the underlying of these future contracts is the Physical Electricity Index determined daily by EPEX Spot Exchange for base and peak load profiles. To be more specific, the Phelix Base contract is

average price of the hours 1 to 24 for electricity traded on spot market, while the Phelix Peak is the average price of the hours 9 to 20 for electricity traded on spot market. EEX offers continuous trading and trade registration of financially fulfilled Phelix Futures, with Day/Weekend Futures, Week Futures, Month Futures, Quarter Futures and Year Futures available.

The time series of Phelix day base and Phelix day peak prices are displayed in Figure 2.2. Phelix day peak exhibit a larger volatility and more pronounced spikes than the Phelix day base. This is not surprising, since the Phelix day peak corresponds to hours with high and variable demand. Both price series exhibit positive skewness and an excess kurtosis of about 1, implying a heavy-tailed unconditional distribution that is skewed to the right.

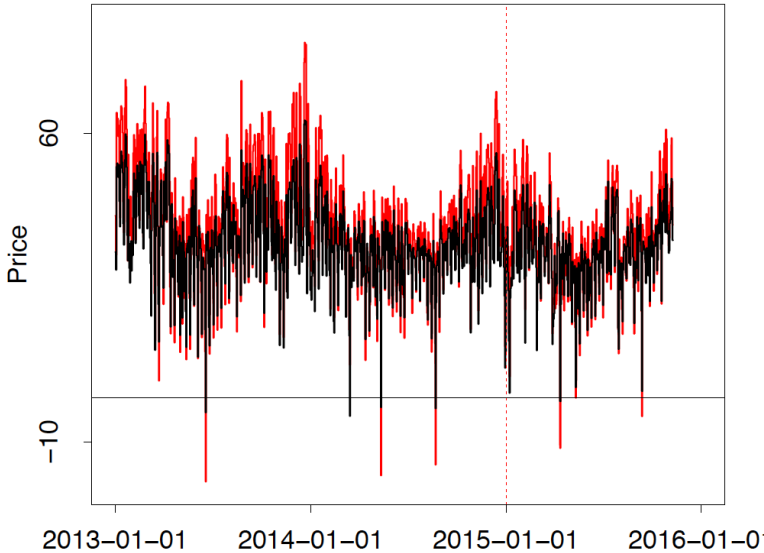


Figure 2.2: Phelix day base (black) and Phelix day peak (red) index from 2013-01-01 to 2015-10-31. The red dotted line marks the end of the in-sample period.

In addition, the Phelix market is also successfully connected to other European power markets. The products of Location Spread enables members to trade price differences between markets, thus enabling participants to benefit from improved liquidity and tighter spreads, for instance, Phelix / French Power, Italian / Phelix Power, Phelix / Nordic Power and Phelix



/ Swiss Power. For the empirical work of this paper, we use the Phelix Future data to find price drivers and important variables in the big system we construct. The decision-making mechanism of energy companies will also be explored.

### 3 THEORETICAL FRAMEWORK

#### 3.1 MODEL DESCRIPTION

We have access to spot prices, trading prices of different future contracts. An interesting question is how all these prices interact with each other? Which variables are crucial for the whole system? To answer this question, we are going to build a Vector Autoregressive Model. However, due to the large number of variables in the system, some sparsity assumption must be imposed for the sake of an accurate estimate. The large dimension comes from two parts:

1. varieties of power derivative products;
2. large lag in VAR model to avoid the correlation of error terms.

The VAR( $p$ ) model (VAR model of order  $p$ ) is constructed according to Lütkepohl (2005),

$$\begin{aligned} y_t &= \nu + A_1 y_{t-1} + A_2 y_{t-2} + \dots + A_p y_{t-p} + u_t \\ &= \nu + (A_1, A_2, \dots, A_p) \left( y_{t-1}^\top, y_{t-2}^\top, \dots, y_{t-p}^\top \right)^\top + u_t \end{aligned} \quad (3.1)$$

where  $y_t = (y_{1t}, y_{2t}, \dots, y_{Kt})^\top$  is a  $(K \times 1)$  random vector consisting  $K$  prices we have at time  $t$ ,  $t$  from 1 to  $T$ .  $A_i$  are fixed  $(K \times K)$  coefficient matrices.  $\nu$  is a  $(K \times 1)$  vector of intercept terms,  $p$  is lag and  $u_t = (u_{1t}, u_{2t}, \dots, u_{Kt})^\top$  is a  $K$ -dimensional innovation process.

The coefficients  $\nu, A_1, \dots, A_p$  are assumed to be unknown in the following. The time series

data  $y_1, y_2, \dots, y_T$  of the  $y$  variable is available and will be used to estimate the coefficients. The multiple time series data will be partitioning into sample and presample values to facilitate the following analysis. Define

$$\begin{aligned}
Y &= (y_1, y_2, \dots, y_T) \\
B &= (v, A_1, A_2, \dots, A_p) \\
Z_t &= (1, y_t, y_{t-p+1})^\top \\
Z &= (Z_0, Z_1, \dots, Z_{T-1})
\end{aligned} \tag{3.2}$$

Hence for multivariate case, the model described in equation (3.1) can also be rewritten as

$$Y = BZ + U \tag{3.3}$$

where  $U = (u_1, u_2, \dots, u_T)$ . The compact form (3.3) is equivalent to

$$\text{vec}(Y) = (Z^\top \otimes I_K) \text{vec}(B) + \text{vec}(U) \tag{3.4}$$

If the vector of intercept terms  $v$  is assumed to be zero, we can thus conclude that the total dimension of the model to be estimated is  $pK^2$  and the total number of observations is  $KT$ .

The ration  $\frac{Kp}{T}$  could be large due to the reasons mentioned earlier, which deteriorates the accuracy of final estimate. Worse still, if  $Kp > T$ , the model is not identified with traditional method. Therefore, we use variable selection technique, such as lasso, to estimate the model. Besides, under normal assumption of error term, the upper bound of error in estimation is positively correlated in  $\frac{\log(K^2p)}{T}$ , part of oracle inequality. the estimation results can be further developed by adding one more step of sure independence screening (SIS hence-after) before variable selection step. Another advantage of SIS is that it could mitigate the problem caused by multicollinearity, which is common in time series setting. The methodologies introduced in the proceeding paragraph are of great importance in the sense that the true underlying model has a sparse representation.

## 3.2 PENALIZED LEAST SQUARE AND VARIABLE SELECTION

Variable selection is an important tool for the linear regression analysis. A popular method is the lasso estimator of Tibshirani (1996), which can be viewed to simultaneously perform model selection and parameter estimation. Related literature includes bridge regression studied by Frank and Friedman (1993) and Fu (1998), the least angle regression of Efron et al. (2004) and adaptive lasso proposed by Zou (2006). Another remarkable example is a smoothly clipped absolute deviation (SCAD) penalty for variable selection proposed by Fan and Li (2001), they proved its oracle properties.

Let us start with consider model estimation and variable selection in a linear regression model,

$$y = X\beta + \varepsilon \tag{3.5}$$

where  $y = (y_1, \dots, y_n)^\top$  is an  $n \times 1$  response vector,  $X = (x_1, \dots, x_p)$  is an  $n \times p$  matrix with  $x_j = (x_{1j}, \dots, x_{nj})^\top$ ,  $j = 1, \dots, p$ .  $\hat{\beta}$  denotes the coefficient estimator produced by the fitting procedure.  $\varepsilon = (\varepsilon_1, \dots, \varepsilon_n)^\top$  is an  $n \times 1$  vector of iid random errors.

The least square estimate is obtained via minimizing  $\|y - X\beta\|^2$ , where the ordinary least squares (OLS) gives nonzero estimates  $\omega = X^\top y$  to all coefficients. Normally best-subset selection are implemented to select significant variables, but the traditional idea of best subset selection methods is computationally too expensive for many statistical applications. Therefore the penalized least square with a penalty term that is separable with respect to the estimated parameter  $\hat{\beta}$  is considered here. In this paper we consider two popular estimators, lasso and SCAD.

The lasso is a regularization technique for simultaneous estimation and variable selection. Its estimate is defined as,

$$\begin{aligned}\hat{\beta}_{LASSO} &= \arg \min_{\beta} \|y - X\beta\|^2 + \lambda \sum_{j=1}^p |\beta_j| \\ &= \arg \min_{\beta} \|y - \sum_{j=1}^p x_j \beta_j\|^2 + \lambda \sum_{j=1}^p |\beta_j|\end{aligned}\quad (3.6)$$

where  $\lambda$  is a tuning parameter. The second term in equation (3.2) is known as the  $\ell_1$ -penalty. The idea behind lasso is the coefficients shrinks toward 0 as  $\lambda$  increase. When  $\lambda$  is sufficiently large, some of the estimated coefficients are exactly zero. The estimation accuracy comes from the trade-off between estimation variance and the bias.

To sum up, lasso is the penalized least square estimates with the  $\ell_1$  penalty in the general least squares and likelihood settings. Furthermore, the  $\ell_2$  penalty results in a ridge regression and  $\ell_p$  penalty will lead to a bridge regression. In the setting of bridge regression, the penalty term is of  $\ell_p$  norm.

We proceed to a brief introduction of the SCAD method. In the present context, the SCAD estimator is given by,

$$\hat{\beta}_{SCAD} = \begin{cases} \text{sgn}(\omega)(|\omega| - \lambda)_+ & \text{when } |\omega| \leq 2\lambda \\ \frac{\{(a-1)\omega - \text{sgn}(\omega)a\lambda\}}{a-2} & \text{when } 2\lambda < |\omega| \leq a\lambda \\ \omega & \text{when } |\omega| > a\lambda \end{cases}\quad (3.7)$$

where  $a > 2$  is an additional tuning parameter. The continuous differentiable penalty function for SCAD estimator is defined by,

$$p'_\lambda(\beta) = \lambda \left\{ I(\beta \leq \lambda) + \frac{(a\lambda - \beta)_+}{(a-1)\lambda} I(\beta > \lambda) \right\} \quad \text{for } a > 2 \text{ and } \beta > 0 \quad (3.8)$$

Both estimators are members of this penalized likelihood family. LASSO has better per-

formance when the noise to signal ratio is large, but this approach creates bias. SCAD can generate variable selection results without generating excess biases.

### 3.3 ITERATED-SIS ESTIMATION

Fan and Lv (2008) proposed a SIS method to select important variables in ultra high-dimensional linear models. The proposed two-stage procedure can perform better than other methods in the sense of statistical learning problems. The SIS method is based on the concept of sure screening, is defined as the correlation learning which filters out the features that have weak correlation with the response. By sure screening, all the important variables survive after variable screening with probability tending to 1.

Fan et al. (2009) improve iterated-SIS to a general pseudo-likelihood framework by allowing feature deletion in the iterative process. Fan et al. (2010) further extend the SIS model and consider an independent learning by ranking the maximum marginal likelihood estimator or maximum marginal likelihood itself for generalized linear models. Here we combine the VAR( $p$ ) model and SIS algorithm to find out the key elements in a big system. The basic idea of SIS is introduced in the following.

Let  $\omega = (\omega_1, \omega_2, \dots, \omega_p)^\top$  be a  $p$ -vector that is obtained by component-wise regression, i.e.,

$$\omega = X^\top y \tag{3.9}$$

where  $y$  is  $n$  vector of response and  $X$  is a  $n \times p$  data matrix.  $\omega$  is a vector of marginal correlations of predictors with the response of predictors with the response variable, rescaled by the standard deviation of the response.

When there are more predictors than observation, LS (least square) estimator is noisy, that's why ridge regression is considered. Let  $\omega^\lambda = (\omega_1^\lambda, \dots, \omega_p^\lambda)^\top$  be a  $p$ -vector obtained

by ridge regression, i.e.,

$$\omega^\lambda = (X^\top X + \lambda I_p)^{-1} X^\top y \quad (3.10)$$

where  $\lambda > 0$  is a regularization parameter. Obviously, when  $\lambda \rightarrow 0$ ,  $\omega^\lambda \rightarrow \hat{\beta}_{LS}$  and  $\lambda \rightarrow \infty$ ,  $\lambda \omega^\lambda \rightarrow \omega$ . The component-wise regression is a specific case of ridge regression with  $\lambda = \infty$ .

The iterated-SIS algorithm applied for estimating the  $VAR(p)$  model is,

1. Apply SIS for initial screening, reduce the dimensionality to a relative large scale  $d$ ;
2. Apply a lower dimensional model selection method (such as lasso, SCAD) to the sets of variables selected by SIS;
3. Apply SIS to the variables selected in the previous step;
4. Repeat step 2 and 3 until the set of selected variables do not decrease.

### 3.4 CONNECTEDNESS MEASURE

The interactions between the variables, i.e., the directional connectedness measure  $\theta_{ij}(q)$  is calculated by the generalized impulse response analysis using the sparse estimation of  $VAR(p)$  models. With iterated-SIS algorithm to estimate the sparse VARs structure, we can acquire its moving average (MA) transformation,

$$y_t = \sum_{i=0}^{\infty} B_i u_{t-i} \quad (3.11)$$

The coefficient matrices  $B_i$  obey  $B_i = \sum_{j=1}^{i-1} B_{i-j} A_j$ , with  $B_0 = I_K$  and  $A_j = 0$  for  $j > p$ .  $A_j, j = 1, 2, \dots, p$  is the coefficient matrices of  $VAR(p)$  model.

Denoting the GFEVD by  $\theta_{ij}(q)$ ,

$$\theta_{ij}(q) = \frac{\sigma_{jj}^{-1} \sum_{q=0}^{Q-1} (e_i^\top \hat{B}_q \Sigma e_j)^2}{\sum_{q=0}^{Q-1} (e_i^\top \hat{B}_q \Sigma \hat{B}_q^\top e_i)} \quad (3.12)$$

where  $q$  is the lag order,  $e_i$  is an  $pK^2 \times 1$  selection vector with unity as its  $i$ -th element and zeros elsewhere.  $\Sigma = E(u_t u_t^\top)$ , is the covariance matrix of the non-orthogonalized VAR( $p$ ) in equation (3.1).  $\sigma_{jj}$  is the corresponding  $j$ -th diagonal element of  $\Sigma$ . The matrices  $\hat{B}_l$  are the estimated coefficient matrices of equation (3.11).

To measure the persistent effect of a shock on the behavior of a series, we aim to acquire the population connectedness table 3.1, according to Diebold and Yilmaz (2014).

	$x_1$	$x_2$	...	$x_n$	From others
$x_1$	$\theta_{11}(q)$	$\theta_{12}(q)$	...	$\theta_{1n}(q)$	$\sum_{j=1}^n \theta_{1j}(q), j \neq 1$
$x_2$	$\theta_{21}(q)$	$\theta_{22}(q)$	...	$\theta_{2n}(q)$	$\sum_{j=1}^n \theta_{2j}(q), j \neq 2$
$\vdots$	$\vdots$	$\vdots$		$\vdots$	$\vdots$
$x_n$	$\theta_{n1}(q)$	$\theta_{n2}(q)$	...	$\theta_{nn}(q)$	$\sum_{j=1}^n \theta_{nj}(q), j \neq n$
To others	$\sum_{i=1}^n \theta_{i1}(q), i \neq 1$	$\sum_{i=1}^n \theta_{i2}(q), i \neq 2$	...	$\sum_{i=1}^n \theta_{in}(q), i \neq n$	$\frac{1}{n} \sum_{i=1, j=1}^n \theta_{ij}(q), i \neq j$

Table 3.1: Connectedness table of interest.

The rightmost column gives the "from" effect of total connectedness, and the bottom row gives the "to" effect. In particular, the directional connectedness "from" and "to" associated with the forecast error variation  $\theta_{ij}$  for specific power contract when the arising shocks transmit from one stock to the others. These two connectedness estimators can be obtained by adding up the row or column elements, the pairwise directional connectedness from  $j$  to  $i$  is given by,

$$C_{i \leftarrow j}^Q = \theta_{ij}(q) \quad (3.13)$$

The total directional connectedness "from"  $C_{i \leftarrow \cdot}$  (others to  $i$ ), "to"  $C_{\cdot \leftarrow j}$  ( $j$  to others) and

the corresponding net connectedness are defined as

$$\begin{aligned}
C_{i \leftarrow \bullet} &= \sum_{j=1}^n \theta_{ij}, i \neq j \\
C_{\bullet \leftarrow j} &= \sum_{i=1}^n \theta_{ij}, i \neq j \\
C_i &= C_{to} - C_{from} = C_{\bullet \leftarrow i} - C_{i \leftarrow \bullet}
\end{aligned} \tag{3.14}$$

## 4 EMPIRICAL STUDY

### 4.1 DATA

As introduced in Section 2, EEX offers continuous trading data of Phelix Futures. The available load profiles are base, peak and off-peak. The available products with different maturities have five kinds, Day/Weekend Futures, Week Futures, Month Futures, Quarter Futures and Year Futures. Nevertheless the products of Day/Weekend Futures and Week Futures only have the off-peak load data, for all other contracts base and peak only. Here we recall the underlying of the Phelix Futures data, the Phelix Base contract is average price of the hours 1 to 24 for electricity traded on spot market, while the Phelix Peak is the average price of the hours 9 to 20 for electricity traded on spot market. Therefore we involve the products of spot prices as well. The contracts of spot prices are diversified in Hours from 00-01h up to 23-24h, and in Blocks of Base Monthly, off-peak 01-08, off-peak 21-24, Peak Monthly. The dataset we constructed is provided by Bloomberg, we have 90 kinds of contracts in total. The time span is from 30.09.2010 to 31.07.2015. All the contracts are listed on Table 4.1 with detailed information in Table 4.2.

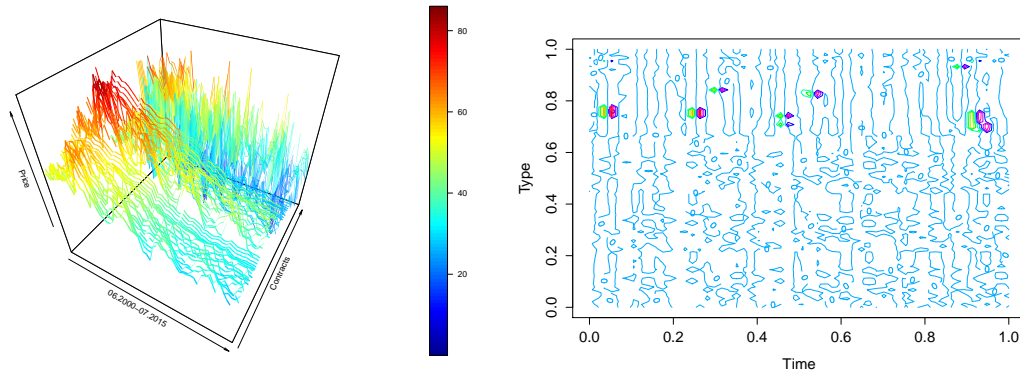
No.	Symbol	Description
1	GI1.Comdty - GI7.Comdty	Phelix Base Month Option, and the respective next six delivery months



2	GT1.Comdty - GT7.Comdty	Phelix Base Quarter Option, and the respective next six delivery quarters
3	HP1.Comdty - HP6.Comdty	Phelix Base Year Option, and the respective next five delivery years
4	GJ1.Comdty - GJ7.Comdty	Phelix Peak Month Future, and the respective next six delivery months
5	HI1.Comdty - HI7.Comdty	Phelix Peak Quarter Future, and the respective next six delivery quarters
6	NE1.Comdty - NE6.Comdty	Phelix Peak Year Future, and the respective next five delivery years
7	POA1.Comdty - POA7.Comdty	Phelix Off-Peak Month Future, and the respective next six delivery months
8	PDA1.Comdty - PDA7.Comdty	Phelix Off-Peak Quarter Future, and the respective next six delivery quarters
9	PBA1.Comdty - PBA6.Comdty	Phelix Off-Peak Year Future, and the respective next five delivery years
10	LPXBHR01.Index LPXBHR24.Index	- EEX Day-ahead Spot Market with Bid Type from 00-01 to 23-24h, e.g. LPXBHR14.Index is EEX Day-ahead Spot price based on bid hours from 13 -14.
11	LPXBHRxx.Index	EEX Day-ahead Spot Market with different Bid Types: LPXBHB.Index is Base Monthly 00-14h; LPXBHOP1.Index is Off Peak1 01-08h; LPXBHOP2.Index is Off Peak2 21-24h; LPXBHP.Index is Peak Monthly 08 - 20h; LPXBHRB.Index is Baseload; LPXBHRP.Index is Peakload.

---

Table 4.2: Selected contracts from the file "Products 2016" provided by European Energy Exchange EEX AG.



(a) Ribbon plot of prices over 90 contracts

(b) Contour plot of log return

Figure 4.1: Overview of dataset

To remove the redundant variable, we apply screening technique to select variables using the Phelix Futures consisting of different contracts and over different maturities. To implement the VAR model, first order difference of the data in Figure 4.1a is needed to transform non-stationary data to stationary time series. The contour plot of the constructed dataset are depicted in Figure 4.1b.

In the market of Phelix Futures, final settlement at negative prices is also possible. There are some missing values after transforming the original data to stationary time series by first order difference. To deal with the missing data in dataset, some quick fixes such as mean-substitution may be fine in some cases. While such simple approaches usually introduce bias into the data, for instance, applying mean substitution leaves the mean unchanged (which is desirable) but decreases variance, which may be undesirable. In our paper, we impute missing values with plausible values drawn from a distribution using an approach proposed by Van Buuren and Oudshoorn (2000).

Symbol	Types			
GI	GI1.Comdty	GI2.Comdty	GI3.Comdty	GI4.Comdty
	GI5.Comdty	GI6.Comdty	GI7.Comdty	
GT	GT1.Comdty	GT2.Comdty	GT3.Comdty	GT4.Comdty
	GT5.Comdty	GT6.Comdty	GT7.Comdty	
HP	HP1.Comdty	HP2.Comdty	HP3.Comdty	HP4.Comdty
	HP5.Comdty	HP6.Comdty		
GJ	GJ1.Comdty	GJ2.Comdty	GJ3.Comdty	GJ4.Comdty
	GJ5.Comdty	GJ6.Comdty	GJ7.Comdty	
HI	HI1.Comdty	HI2.Comdty	HI3.Comdty	HI4.Comdty
	HI5.Comdty	HI6.Comdty	HI7.Comdty	
NE	NE1.Comdty	NE2.Comdty	NE3.Comdty	NE4.Comdty
	NE5.Comdty	NE6.Comdty		
POA	POA1.Comdty	POA2.Comdty	POA3.Comdty	POA4.Comdty
	POA5.Comdty	POA6.Comdty	POA7.Comdty	
PDA	PDA1.Comdty	PDA2.Comdty	PDA3.Comdty	PDA4.Comdty
	PDA5.Comdty	PDA6.Comdty	PDA7.Comdty	
PBA	PBA1.Comdty	PBA2.Comdty	PBA3.Comdty	PBA4.Comdty
	PBA5.Comdty	PBA6.Comdty		
LPXBHR	LPXBHR01.Index	LPXBHR02.Index	LPXBHR03.Index	LPXBHR04.Index
	LPXBHR05.Index	LPXBHR06.Index	LPXBHR07.Index	LPXBHR08.Index
	LPXBHR09.Index	LPXBHR10.Index	LPXBHR11.Index	LPXBHR12.Index
	LPXBHR13.Index	LPXBHR14.Index	LPXBHR15.Index	LPXBHR16.Index
	LPXBHR17.Index	LPXBHR18.Index	LPXBHR19.Index	LPXBHR20.Index
	LPXBHR21.Index	LPXBHR22.Index	LPXBHR23.Index	LPXBHR24.Index
LPXBHxx	LPXBHBMI.Index	LPXBHOP1.Index	LPXBHOP2.Index	LPXBHPMI.Index
	LPXBHRBS.Index	LPXBHRPK.Index		

Table 4.1: Phelix Futures data traded at EEX.

The patterns of missing data for the original dataset and imputation dataset are compared in the Figure 4.2. The distributions of the variables are shown as individual points, the imputed data for each imputed dataset is showed in magenta while the density of the observed data is showed in blue. The distributions are expected to be similar based on the assumption. We can observe that the shape of the magenta points (imputed) matches the shape of the blue ones (observed). The matching shape tells us that the imputed values are indeed plausible values. With the imputed dataset of interest, we proceed to the estimation results derived from the iterated-SIS methodology.

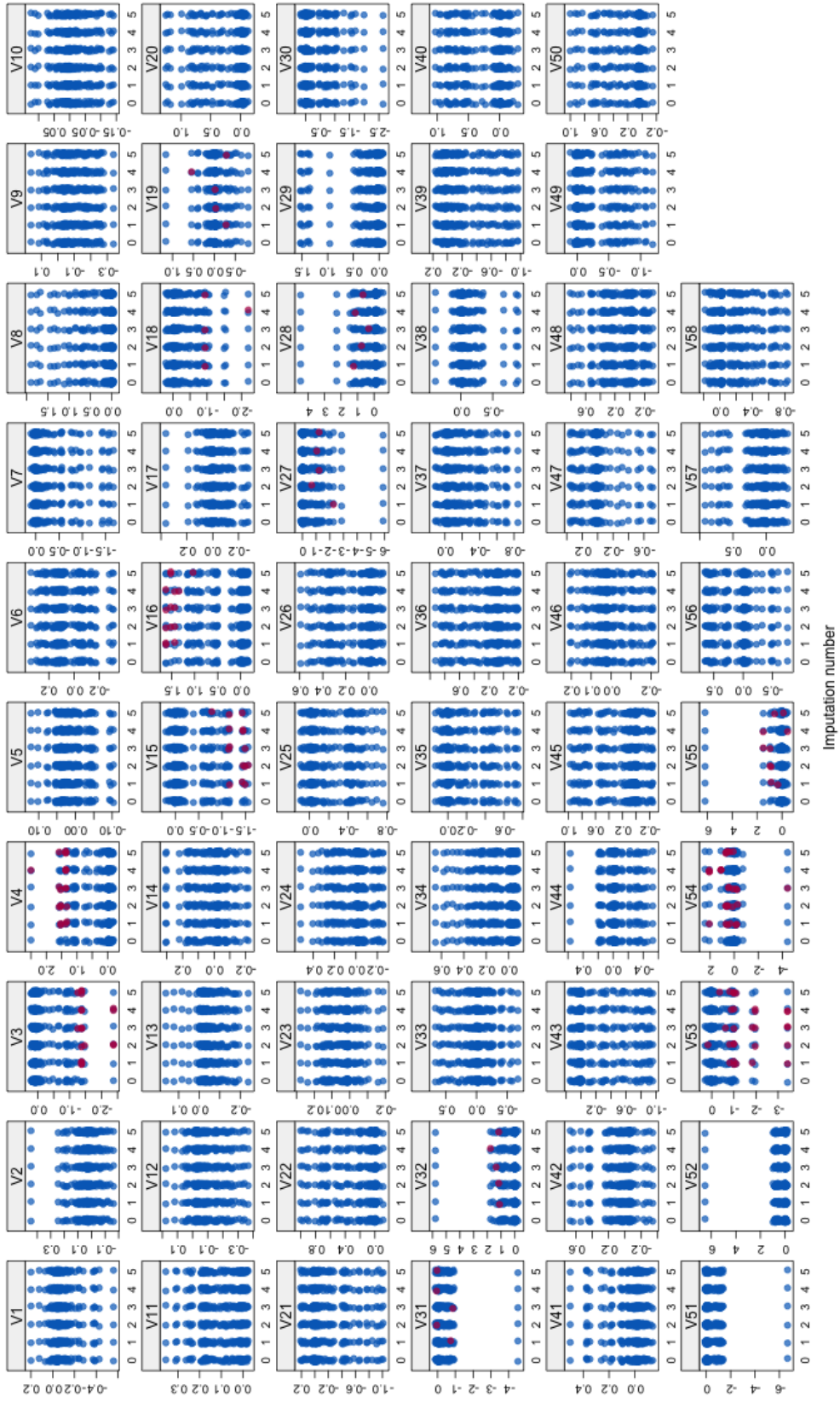


Figure 4.2: Pattern of imputed data.

## 4.2 MODEL SELECTION

With iterated-SIS, we can show the consistency of variable selection. Besides, with only a small set of relevant variables in the final model after iterated-SIS with lasso, the final estimate can be shown to be normally distributed.

Each curve corresponds to a variable. It shows the path of its coefficient against the  $l_1$ -norm of the whole coefficient vector as  $\lambda$  varies. The estimation results are plotted in Figure 4.3, while the iterated-SIS-SCAD output is shown in Figure 4.4.

To estimate the accuracy of forecasting behavior concerning the model selected, the observations  $y_t$  is partitioning into sample and pre-sample values. In this paper we select the pre-sample as 30.09.2010 - 28.11.2014, and the rest is treated as the sample from 31.12.2014 to 07.12.2015. We use different lags for estimating the VAR( $p$ ) model. The lag length for the VAR( $p$ ) model may be determined using model selection criteria. General approach is as follows,

- Fit the VAR( $p$ ) models with different lags  $p = 0, \dots, p_{max}$ ,
- Choose the value of  $p$  which minimizes some model selection criteria.

Model selection criteria for VAR( $p$ ) can be written as,

$$IC(p) = \log|\hat{H}(p)| + \varphi(K, p)c_T \quad (4.1)$$

where  $\varphi(K, p)$  is a penalty function.  $c_T$  is a sequence indexed by the sample size  $T$ . The residual covariance matrix without a degrees of freedom correction is defined as,

$$\hat{H}(p) = \frac{1}{T} \sum_{t=1}^T u_t^\top u_t \quad (4.2)$$

Rewrite equation 4.1 with different penalty functions, the three most common information

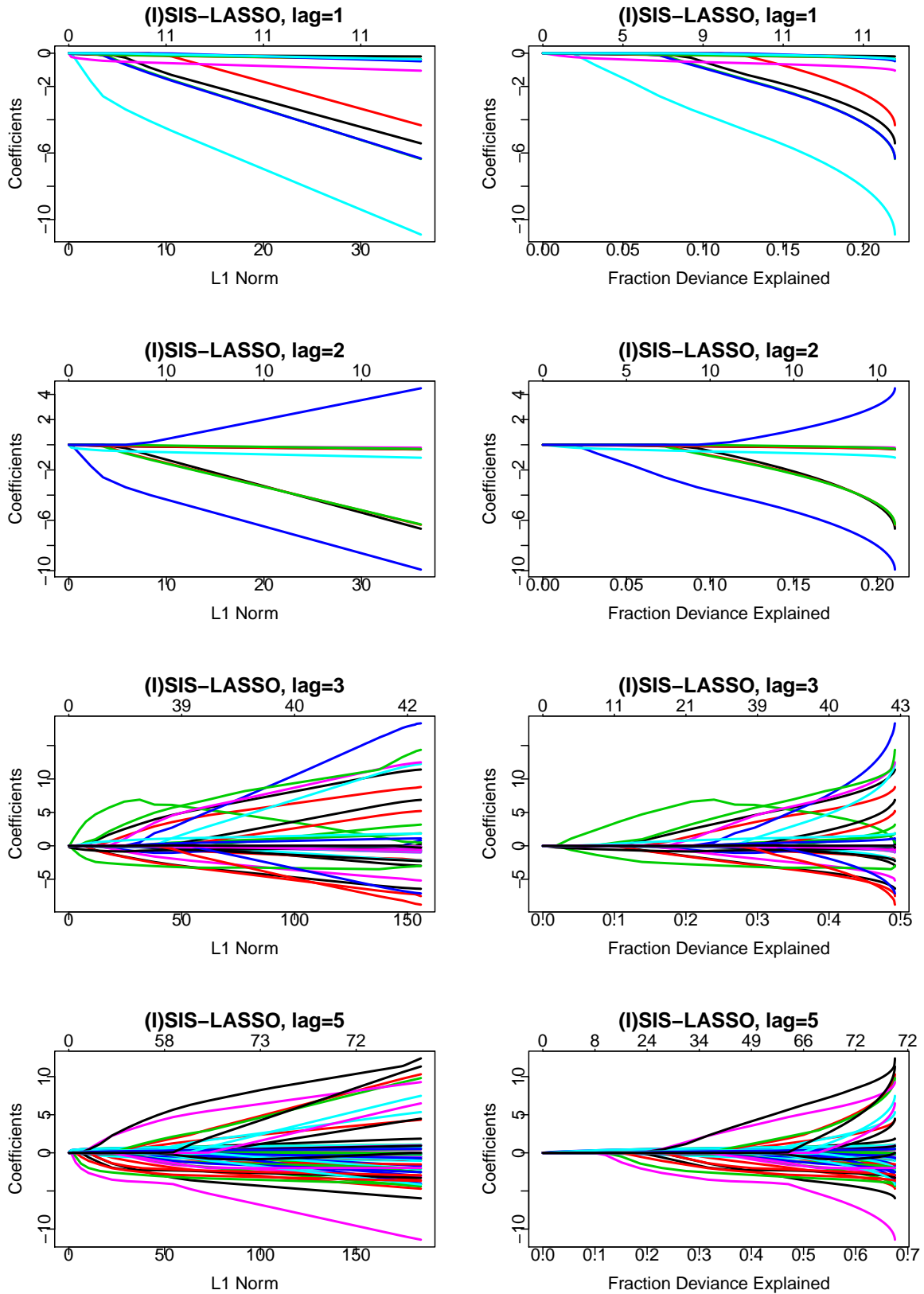


Figure 4.3: iterated-SIS-LASSO estimation results.

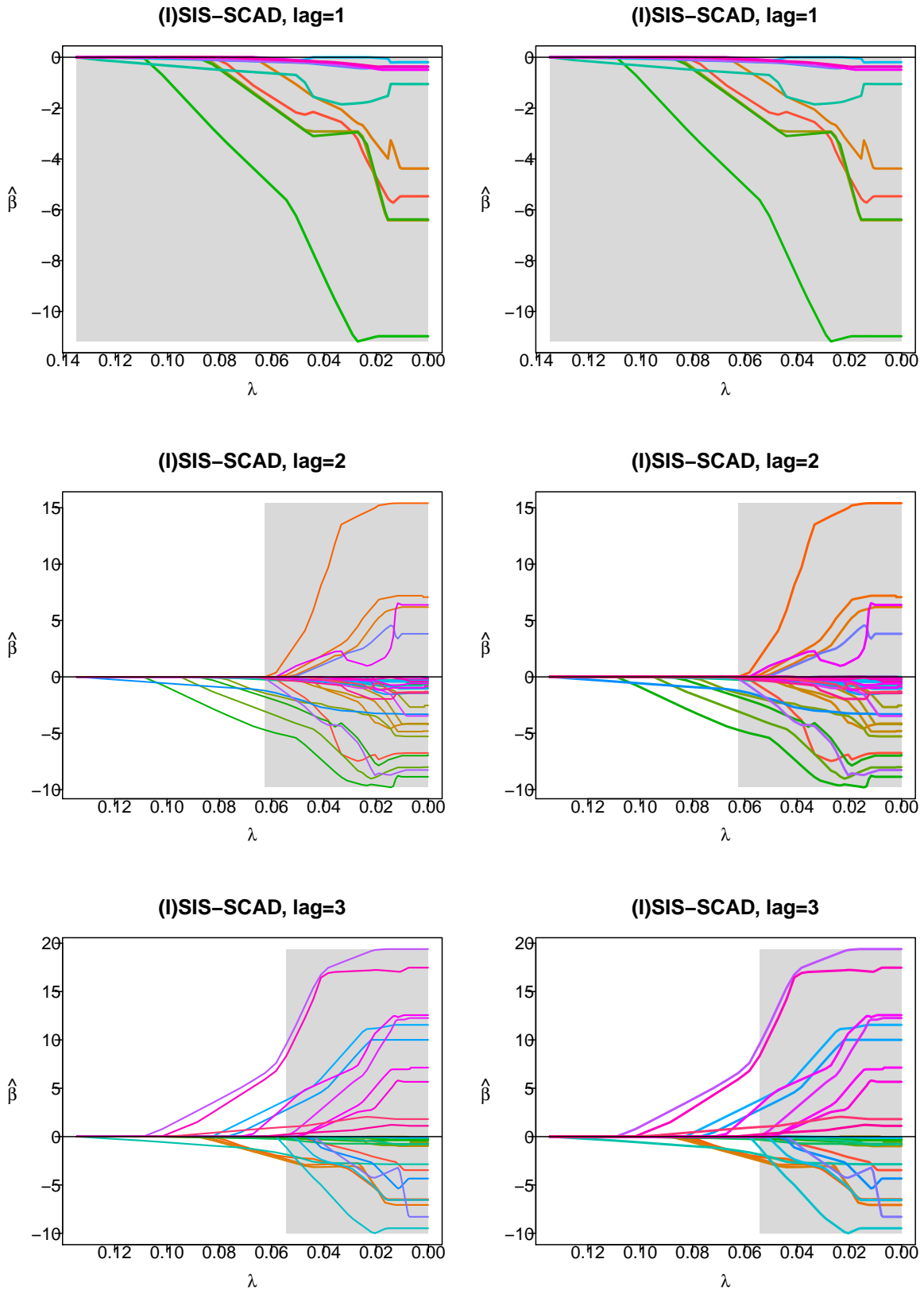


Figure 4.4: iterated-SIS-SCAD estimation results.

Model	AIC	HQ(C)	BIC
iterated-SIS-lasso, $p = 1$	4.5686	4.7249	5.7864
iterated-SIS-lasso, $p = 2$	4.5006	4.6426	5.6076
iterated-SIS-lasso, $p = 3$	7.7034	8.3143	12.4637
iterated-SIS-lasso, $p = 5$	7.0839	8.1209	15.1652
iterated-SIS-SCAD, $p = 1$	4.5714	4.7277	5.7892
iterated-SIS-SCAD, $p = 2$	6.1043	6.1043	9.5782
iterated-SIS-SCAD, $p = 3$	7.2559	7.6820	10.5770

Table 4.3: Model Selection Results according to the Akaike (AIC), Schwarz-Bayesian (BIC) and Hannan-Quinn (HQ) criteria.

criteria are the Akaike (AIC), Schwarz-Bayesian (BIC) and Hannan-Quinn (HQ),

$$AIC = \log|\hat{H}(p)| + \frac{2}{T}pK^2 \quad (4.3)$$

$$HQ = \log|\hat{H}(p)| + \frac{2\log\log T}{T}pK^2 \quad (4.4)$$

$$BIC = \log|\hat{H}(p)| + \frac{\log T}{T}pK^2 \quad (4.5)$$

The model selection results are shown in Table 4.3. The most common information criteria: the Akaike (AIC), Schwarz-Bayesian (BIC) and Hannan-Quinn (HQ) criteria are compared. One observe that the model using the Iterated-SIS-lasso and  $p = 2$  performs at best.

Recall equation 3.1, the VAR( $p$ ) model,

$$\begin{aligned} y_t &= v + A_1 y_{t-1} + A_2 y_{t-2} + \dots + A_p y_{t-p} + u_t \\ &= v + (A_1, A_2, \dots, A_p) \left( y_{t-1}^\top, y_{t-2}^\top, \dots, y_{t-p}^\top \right)^\top + u_t \end{aligned}$$

We select the in-sample dataset as 30.09.2010-28.11.2014, the out-of-sample dataset used to measure model performance is from 31.12.2014 to 31.07.2015. We roll each model through the out-of-sample data set one observation at a time while each time forecasting the target



Lag	iterated-SIS-lasso	iterated-SIS-SCAD
$p = 1$	0.0697	0.0697
$p = 2$	<b>0.0670</b>	0.0701
$p = 3$	1.9598	0.1413
$p = 5$	0.1397	-

Table 4.4: MSE of out-of-sample forecasting during 31.12.2014 - 31.07.2015

variable one month ahead. By rolling window. The mean squared errors (MSE) for different models are calculated and reported in Table 4.4. VAR(2) with iterated-SIS-lasso technique performs best.

### 4.3 NETWORK ANALYSIS

We estimate VAR models using the iterated-SIS algorithm as described in previous section. Then we compute variance decompositions and corresponding connectedness measures at horizon  $H = 10$ , using the estimated VAR parameters.

### 4.4 FULL-SAMPLE CONNECTEDNESS

The graph of our full-sample energy market network is depicted in Figure 4.5. We observe the cluster phenomena in this graph, which motivates us to study the connectedness between contracts within and across 11 different kinds of energy contracts. In general, the contracts that belong to the same type tend to appear inside the same cluster. We find out several pairs of strong connections between different types of contracts, for example, the upper-left area reveals that the LPXBHR-type and LPXBHxx-type are massively connected. In addition, a cluster consisting of HP-type (Phelix Base Year Future), NE-type (Phelix Peak Year Future) and PBA-type (Phelix Off-Peak Year Future) indicates the closer relationship among these contracts, this implies the year futures are closer to each other while the week

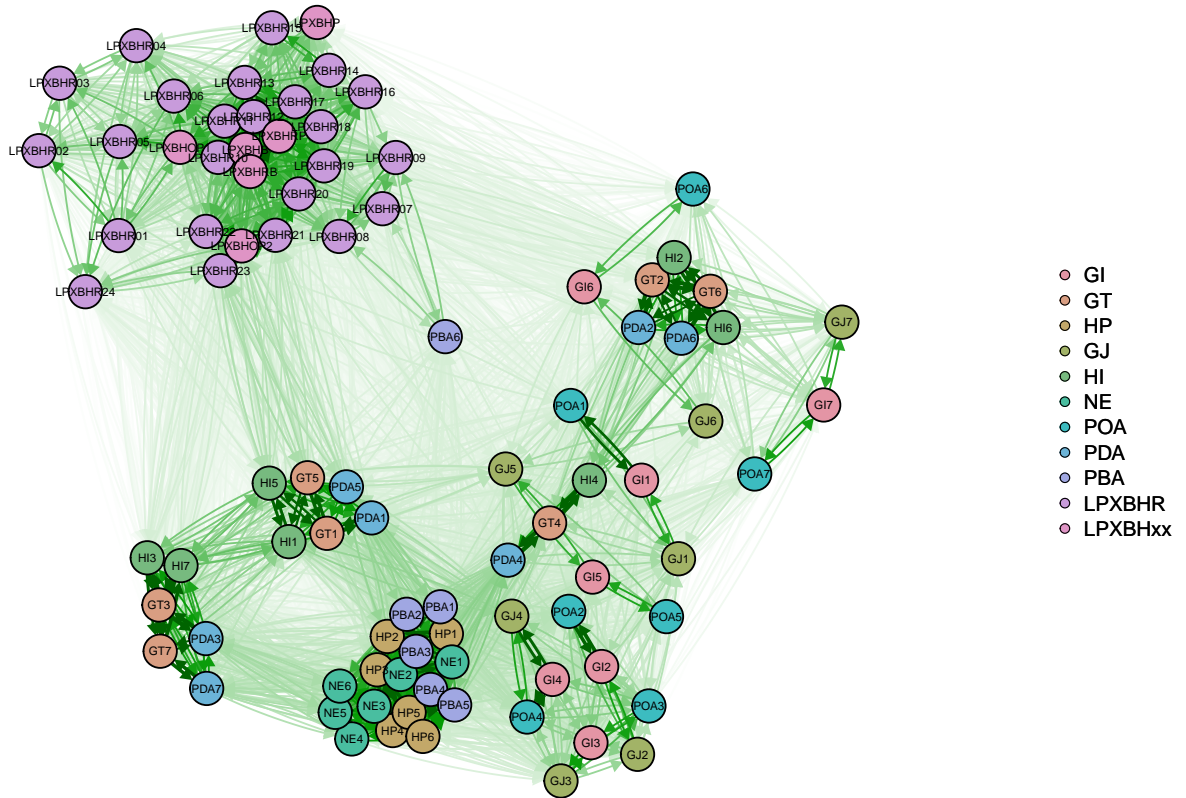


Figure 4.5: The graph for full-sample energy market network, across 11 different kinds with in total 90 contracts.

future and quarter future remain distinct.

Table 4.5 summarizes the full-sample connectedness of German power market across 11 different power contract types, with the own effects equal to the diagonal elements. We observe the contracts that have significant impacts are the "From" impact of "LPXBHR"-type and "To" impact of "HP"-type. The strongest link is the impact of LPXBHxx-type on the LPXBHR, however the inverse impact does not exist. Furthermore, HP-type contracts have stronger links from and to the other contract types. We can also conclude that the total impacts are mainly distributed among three types of contracts, i.e., HP-type, NE-type and PBA-type. The main risk of the whole market is mainly caused by LPXBHxx-type, HP-

	GI	GT	HP	GJ	HI	NE	POA	PDA	PBA	LPXBHR	LPXBHxx	From
GI	1.75	0.46	0.86	1.46	0.44	0.71	1.48	0.48	0.80	0.15	0.15	8.74
GT	0.46	2.33	0.98	0.58	2.41	0.93	0.42	2.03	0.84	0.30	0.41	11.70
HP	0.73	0.84	5.27	0.63	0.51	4.78	0.70	1.21	4.19	0.06	0.03	18.95
GJ	1.46	0.58	0.73	1.80	0.63	0.64	1.09	0.51	0.65	0.13	0.13	8.36
HI	0.44	2.41	0.60	0.63	2.65	0.63	0.37	1.92	0.49	0.34	0.48	10.96
NE	0.61	0.79	4.78	0.55	0.54	5.09	0.55	1.05	3.34	0.08	0.12	17.52
POA	1.48	0.42	0.81	1.09	0.37	0.64	1.60	0.48	0.79	0.19	0.18	8.04
PDA	0.48	2.03	1.42	0.51	1.92	1.23	0.48	1.99	1.27	0.26	0.32	11.91
PBA	0.68	0.72	4.19	0.56	0.42	3.34	0.67	1.09	3.88	0.20	0.12	15.88
LPXBHR	0.80	1.24	0.50	0.67	1.35	0.50	0.90	1.12	1.01	7.86	9.81	25.79
LPXBHxx	0.13	0.35	0.03	0.11	0.41	0.12	0.16	0.28	0.13	2.70	3.86	8.28
To	9.03	12.18	20.17	8.59	11.65	18.62	8.41	12.16	17.38	12.28	15.63	146.12
Net	0.29	0.48	1.22	0.23	0.70	1.10	0.37	0.25	1.50	-13.50	7.35	

Table 4.5: Population connectedness table for 11 kinds of contracts.

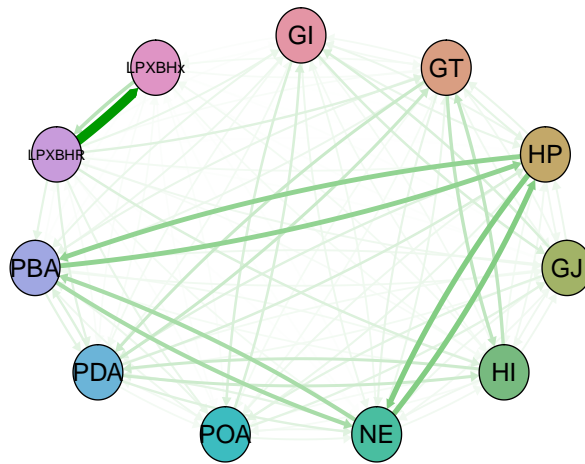


Figure 4.6: The graph for network across 11 different contract types.

type and NE-type. This is potentially interesting because, although HP-type, NE-type are important for the whole market as shown in Figure 4.6, their net connectedness are negligible, with 4.52% and 4.08% of the total market power contracts.

#### 4.5 DETERMINING SIGNIFICANT MARKET COMPONENT

In terms of magnitude for individual power contract reported in Table 4.5, the net directional connectedness from others is distributed rather tightly, in total 77.21% of "LPXBHR"-type and "LPXBHxx"-type.

	LPXBHR01	LPXBHR02	LPXBHR03	LPXBHR04	LPXBHR05	LPXBHR06	LPXBHR07	LPXBHR08
LPXBHR01	1.00	0.71	0.52	0.35	0.53	0.43	0.13	0.14
LPXBHR02	0.42	0.59	0.47	0.36	0.31	0.18	0.06	0.07
LPXBHR03	0.27	0.41	0.54	0.42	0.36	0.23	0.12	0.12
LPXBHR04	0.19	0.32	0.41	0.53	0.38	0.25	0.21	0.15
LPXBHR05	0.25	0.24	0.30	0.33	0.47	0.37	0.19	0.15
LPXBHR06	0.18	0.12	0.18	0.18	0.34	0.41	0.22	0.23
LPXBHR07	0.10	0.08	0.13	0.20	0.22	0.29	0.45	0.40
LPXBHR08	0.10	0.08	0.13	0.14	0.18	0.30	0.45	0.54
LPXBHR09	0.11	0.08	0.14	0.15	0.18	0.35	0.58	0.70
LPXBHR10	0.25	0.23	0.23	0.33	0.49	0.66	0.46	0.49
LPXBHR11	0.27	0.28	0.26	0.35	0.50	0.61	0.42	0.46
LPXBHR12	0.26	0.29	0.23	0.30	0.42	0.48	0.28	0.31
LPXBHR13	0.23	0.30	0.24	0.30	0.39	0.45	0.21	0.27
LPXBHR14	0.16	0.15	0.17	0.23	0.26	0.30	0.13	0.13
LPXBHR15	0.22	0.18	0.17	0.19	0.22	0.27	0.14	0.13
LPXBHR16	0.07	0.06	0.10	0.13	0.19	0.34	0.36	0.41
LPXBHR17	0.13	0.13	0.18	0.22	0.35	0.51	0.29	0.36
LPXBHR18	0.13	0.11	0.15	0.20	0.32	0.47	0.24	0.27
LPXBHR19	0.15	0.11	0.12	0.24	0.32	0.45	0.33	0.30
LPXBHR20	0.10	0.07	0.08	0.17	0.24	0.38	0.32	0.28
LPXBHR21	0.06	0.07	0.05	0.12	0.17	0.28	0.27	0.25
LPXBHR22	0.11	0.13	0.11	0.12	0.19	0.31	0.23	0.26
LPXBHR23	0.10	0.12	0.06	0.07	0.11	0.18	0.12	0.14
LPXBHR24	0.00	0.00	0.01	0.01	0.01	0.00	0.00	0.00
	LPXBHR09	LPXBHR10	LPXBHR11	LPXBHR12	LPXBHR13	LPXBHR14	LPXBHR15	LPXBHR16
LPXBHR01	0.16	0.25	0.27	0.26	0.23	0.13	0.08	0.03
LPXBHR02	0.07	0.15	0.19	0.20	0.21	0.07	0.04	0.03
LPXBHR03	0.10	0.13	0.14	0.13	0.14	0.07	0.05	0.05
LPXBHR04	0.12	0.21	0.23	0.20	0.20	0.11	0.10	0.15
LPXBHR05	0.12	0.24	0.25	0.22	0.21	0.11	0.08	0.11
LPXBHR06	0.20	0.29	0.27	0.23	0.22	0.13	0.12	0.15
LPXBHR07	0.38	0.27	0.26	0.20	0.16	0.09	0.09	0.16
LPXBHR08	0.53	0.28	0.27	0.19	0.17	0.08	0.08	0.09
LPXBHR09	0.73	0.33	0.31	0.22	0.19	0.10	0.11	0.09
LPXBHR10	0.45	0.98	0.94	0.82	0.70	0.43	0.37	0.43
LPXBHR11	0.43	0.94	0.98	0.92	0.81	0.44	0.37	0.43
LPXBHR12	0.31	0.84	0.94	1.00	0.90	0.46	0.36	0.44
LPXBHR13	0.27	0.71	0.83	0.90	1.00	0.62	0.51	0.43
LPXBHR14	0.13	0.39	0.41	0.41	0.54	0.83	0.77	0.27
LPXBHR15	0.14	0.31	0.32	0.30	0.40	0.67	0.71	0.27
LPXBHR16	0.41	0.39	0.38	0.34	0.32	0.22	0.26	0.59
LPXBHR17	0.33	0.68	0.72	0.72	0.78	0.50	0.51	0.65

LPXBHR18	0.24	0.66	0.66	0.65	0.70	0.48	0.50	0.71
LPXBHR19	0.27	0.63	0.63	0.60	0.63	0.48	0.47	0.62
LPXBHR20	0.26	0.64	0.61	0.58	0.52	0.34	0.32	0.49
LPXBHR21	0.24	0.56	0.54	0.53	0.44	0.25	0.22	0.35
LPXBHR22	0.24	0.51	0.47	0.42	0.35	0.17	0.14	0.32
LPXBHR23	0.14	0.40	0.41	0.44	0.39	0.22	0.17	0.27
LPXBHR24	0.00	0.03	0.04	0.07	0.07	0.02	0.01	0.03
	LPXBHR17	LPXBHR18	LPXBHR19	LPXBHR20	LPXBHR21	LPXBHR22	LPXBHR23	LPXBHR24
LPXBHR01	0.13	0.13	0.15	0.10	0.06	0.11	0.10	0.00
LPXBHR02	0.08	0.07	0.08	0.07	0.14	0.17	0.22	0.38
LPXBHR03	0.09	0.08	0.07	0.06	0.11	0.12	0.15	0.42
LPXBHR04	0.16	0.16	0.18	0.15	0.17	0.16	0.18	0.36
LPXBHR05	0.17	0.15	0.16	0.14	0.19	0.18	0.22	0.50
LPXBHR06	0.22	0.20	0.21	0.19	0.25	0.24	0.27	0.55
LPXBHR07	0.20	0.19	0.23	0.22	0.20	0.18	0.16	0.17
LPXBHR08	0.20	0.16	0.18	0.18	0.21	0.20	0.17	0.20
LPXBHR09	0.24	0.17	0.20	0.19	0.17	0.18	0.10	0.00
LPXBHR10	0.67	0.65	0.61	0.63	0.55	0.50	0.39	0.04
LPXBHR11	0.71	0.65	0.62	0.60	0.53	0.46	0.40	0.05
LPXBHR12	0.72	0.65	0.61	0.58	0.53	0.42	0.43	0.08
LPXBHR13	0.78	0.70	0.63	0.52	0.44	0.35	0.39	0.08
LPXBHR14	0.42	0.41	0.41	0.30	0.22	0.16	0.21	0.07
LPXBHR15	0.38	0.37	0.36	0.25	0.18	0.13	0.15	0.05
LPXBHR16	0.46	0.46	0.42	0.36	0.28	0.26	0.20	0.02
LPXBHR17	1.00	0.93	0.74	0.62	0.46	0.36	0.27	0.02
LPXBHR18	0.93	1.00	0.83	0.68	0.46	0.38	0.30	0.02
LPXBHR19	0.74	0.83	1.00	0.81	0.59	0.45	0.46	0.05
LPXBHR20	0.62	0.68	0.81	1.00	0.82	0.64	0.56	0.08
LPXBHR21	0.46	0.46	0.59	0.82	1.00	0.82	0.71	0.27
LPXBHR22	0.36	0.38	0.45	0.64	0.82	1.00	0.81	0.23
LPXBHR23	0.27	0.30	0.46	0.56	0.71	0.81	1.00	0.38
LPXBHR24	0.03	0.03	0.06	0.08	0.22	0.19	0.31	0.82

Table 4.6: Population connectedness table for LPXBHR contracts.

We start with directional connectedness across 24 contracts of "LPXBHR"-type in Table 4.6. Some blocks of high connectedness are detected, especially for the trading hours ranging from 9-13h and 16-19h. Table 4.7 provides the "from", "to" and "net" effects for 24 contracts in descending order of importance. Our finding clearly shows that, the impact from day-ahead spot power contracts that bidding between 9am and 13am are more relevant to the stability of the German power market.

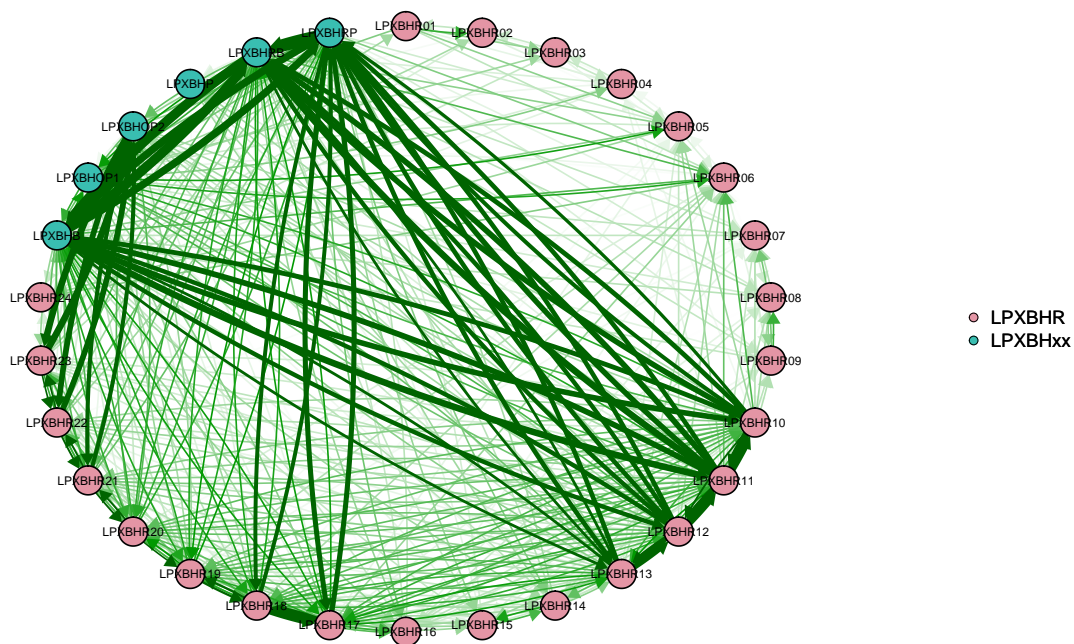


Figure 4.7: The network graph for "LPXBHR"-type and "LPXBHxx"-type power contracts.

Power Contract	From	To	Net
LPXBHR11.Index	12.48	11.08	-1.40
LPXBHR10.Index	12.27	10.83	-1.45
LPXBHR12.Index	11.83	10.55	-1.27
LPXBHR13.Index	11.55	10.28	-1.27
LPXBHR17.Index	11.46	10.05	-1.41
LPXBHR19.Index	11.27	10.05	-1.23
LPXBHR18.Index	11.06	9.79	-1.27
LPXBHR20.Index	10.61	9.73	-0.88
LPXBHR21.Index	9.51	9.31	-0.19
LPXBHR22.Index	8.77	8.51	-0.26
LPXBHR23.Index	7.80	8.48	0.68
LPXBHR14.Index	7.48	8.16	0.68
LPXBHR16.Index	7.02	7.16	0.14
LPXBHR15.Index	6.51	7.15	0.64
LPXBHR01.Index	5.99	6.99	0.99
LPXBHR09.Index	5.64	6.54	0.90
LPXBHR06.Index	5.60	6.42	0.83
LPXBHR05.Index	5.35	6.30	0.94
LPXBHR04.Index	5.28	6.19	0.91
LPXBHR08.Index	5.13	5.65	0.52
LPXBHR07.Index	5.04	4.98	-0.06
LPXBHR02.Index	4.66	4.87	0.21
LPXBHR03.Index	4.36	4.85	0.49
LPXBHR24.Index	2.07	4.84	2.77

Table 4.7: Summary of "From", "To" and "Net" effects across "LPXBHR" contracts bidding from 0h to 24h.

The pairwise directional impacts between "LPXBHR"-type and "LPXBHxx"-type are plotted in Figure 4.7, we find a risk cluster of "LPXBHR10", "LPXBHR11", "LPXBHR11", "LPXBHR12", "LPXBHRP", "LPXBHRB" and "LPXBHB", the graph exhibits strong mutual links between some of the spot contracts. The "LPXBHB" (Base hours 00:00 - 24:00) has significant impacts on the spot contracts from hours 09 to 13, while the impacts from "LPXBHP" (Peak Hours 08:00 - 20:00) is negligible. In addition, both "LPXBHRB" (Baseload) and "LPXBHRP" (Peakload) exhibits strong interconnectedness with the spot contracts from hours 09 to 13. However only the "LPXBHRP" affects the spot prices from hours 16h to 18h. We can infer that the Base spot contract "LPXBHB" is the largest risk contributor due to the strong linkage to the other spot contracts.

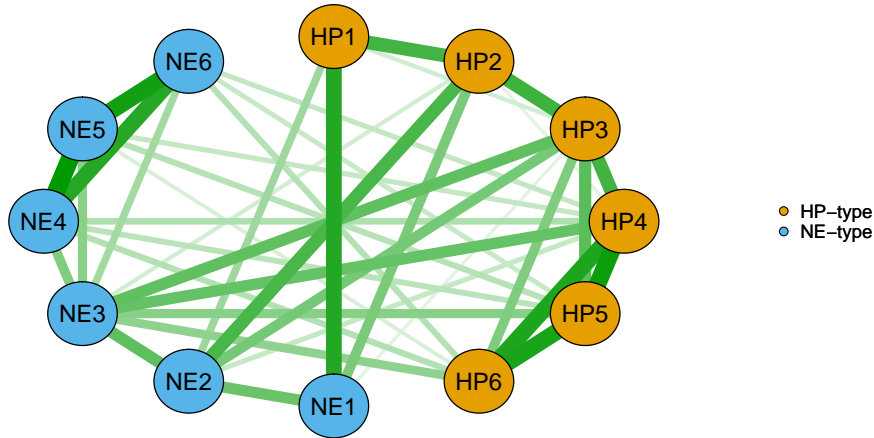


Figure 4.8: The network graph for "HP" and "NE"-type power contracts.

The network graph in Figure 4.8 illustrates the directional connectedness between "HP"-type and "NE"-type power contracts. Compared with Figure 4.5, we can see that, the links between these two types are obviously very strong. "NE" contracts are the Year Futures with maturities up to six years, the underlying of these contracts is the average price of hours 9 to 20 for electricity traded on the spot market. "HP" contracts are the European style options on the Phelix Base Future provided by EEX, the underlying of Phelix Base is the average price of the hours 1 to 24 for electricity traded on the spot market. It is calculated for all calendar days of the year as the simple average of the Auction prices for the hours 1 to 24 in the market area Germany / Austria. This figure shows the similar connectedness pattern between "HP1" and "NE1" contracts.

## 5 CONCLUSION

In this paper we propose a regularization approach for network modeling of German energy market. We combine high-dimensional variable selection techniques with dynamic networks (following the Dieboldt-Yilmaz tradition). By comparing our empirical findings,



we could be able to identify the relevant risk drivers from the portfolio that are unknown to the power market investors. The selection of important market drivers via iterated-SIS algorithm enables us to investigate an ultra high-dimensional portfolio, since the number of parameters to estimate increases quadratically in the number of variables included in the context of VAR estimation.

The results show that contracts like Phelix Base Year Options and Phelix Peak Year Futures are in the core of the Energy futures market. With the wide range of power derivative contracts trading in the German electricity market, we are able to identify, estimated the risk contribution of individual power contract, this helps us to have a better understanding of the German power market functioning and environment.

## REFERENCES

- Acharya, V., Engle, R., and Richardson, M. (2012). Capital shortfall: A new approach to ranking and regulating systemic risks. *The American Economic Review*, 102(3):59–64.
- Acharya, V. V., Pedersen, L. H., Philippon, T., and Richardson, M. (2017). Measuring systemic risk. *The Review of Financial Studies*, 30(1):2–47.
- Babus, A. (2016). The formation of financial networks. *The RAND Journal of Economics*, 47(2):239–272.
- Basu, S., Michailidis, G., et al. (2015). Regularized estimation in sparse high-dimensional time series models. *The Annals of Statistics*, 43(4):1535–1567.
- Bickel, P. J., Ritov, Y., and Tsybakov, A. B. (2009). Simultaneous analysis of lasso and dantzig selector. *Ann. Statist.*, 37(4):1705–1732.
- Brownlees, C. and Engle, R. F. (2016). Srisk: A conditional capital shortfall measure of systemic risk. *The Review of Financial Studies*, 30(1):48–79.
- Candes, E. and Tao, T. (2007). The dantzig selector: Statistical estimation when  $p$  is much larger than  $n$ . *The Annals of Statistics*, pages 2313–2351.
- Demirer, M., Diebold, F. X., Liu, L., and Yilmaz, K. (2017). Estimating global bank network connectedness. Technical report, National Bureau of Economic Research.
- Diebold, F. X. and Yilmaz, K. (2014). On the network topology of variance decompositions: Measuring the connectedness of financial firms. *Journal of Econometrics*, 182(1):119–134.
- Efron, B., Hastie, T., Johnstone, I., Tibshirani, R., et al. (2004). Least angle regression. *The Annals of statistics*, 32(2):407–499.
- Fan, J. and Li, R. (2001). Variable selection via nonconcave penalized likelihood and its oracle properties. *Journal of the American statistical Association*, 96(456):1348–1360.

- Fan, J. and Lv, J. (2008). Sure independence screening for ultrahigh dimensional feature space. *Journal of the Royal Statistical Society: Series B (Statistical Methodology)*, 70(5):849–911.
- Fan, J., Samworth, R., and Wu, Y. (2009). Ultrahigh dimensional feature selection: beyond the linear model. *Journal of Machine Learning Research*, 10(Sep):2013–2038.
- Fan, J., Song, R., et al. (2010). Sure independence screening in generalized linear models with np-dimensionality. *The Annals of Statistics*, 38(6):3567–3604.
- Frank, L. E. and Friedman, J. H. (1993). A statistical view of some chemometrics regression tools. *Technometrics*, 35(2):109–135.
- Fu, W. J. (1998). Penalized regressions: the bridge versus the lasso. *Journal of computational and graphical statistics*, 7(3):397–416.
- Giglio, S., Kelly, B., and Pruitt, S. (2016). Systemic risk and the macroeconomy: An empirical evaluation. *Journal of Financial Economics*, 119(3):457–471.
- Hautsch, N., Schaumburg, J., and Schienle, M. (2014). Financial network systemic risk contributions. *Review of Finance*, 19(2):685–738.
- Kock, A. B. and Callot, L. (2015). Oracle inequalities for high dimensional vector autoregressions. *Journal of Econometrics*, 186(2):325–344.
- Koop, G., Pesaran, M. H., and Potter, S. M. (1996). Impulse response analysis in nonlinear multivariate models. *Journal of econometrics*, 74(1):119–147.
- Loh, P.-L. and Wainwright, M. J. (2011). High-dimensional regression with noisy and missing data: Provable guarantees with non-convexity. In *Advances in Neural Information Processing Systems*, pages 2726–2734.
- Lütkepohl, H. (2005). *New introduction to multiple time series analysis*. Springer Science & Business Media.

- Pesaran, H. H. and Shin, Y. (1998). Generalized impulse response analysis in linear multivariate models. *Economics letters*, 58(1):17–29.
- Tibshirani, R. (1996). Regression shrinkage and selection via the lasso. *Journal of the Royal Statistical Society. Series B*, 58(1):pp. 267–288.
- Van Buuren, S. and Oudshoorn, C. (2000). Multivariate imputation by chained equations. *MICE VI. 0 user's manual. Leiden: TNO Preventie en Gezondheid*.
- Wu, W.-B., Wu, Y. N., et al. (2016). Performance bounds for parameter estimates of high-dimensional linear models with correlated errors. *Electronic Journal of Statistics*, 10(1):352–379.
- Zou, H. (2006). The adaptive lasso and its oracle properties. *Journal of the American statistical association*, 101(476):1418–1429.
- Zou, H. and Hastie, T. (2005). Regularization and variable selection via the elastic net. *Journal of the Royal Statistical Society: Series B (Statistical Methodology)*, 67(2):301–320.

# IRTG 1792 Discussion Paper Series 2018

For a complete list of Discussion Papers published, please visit [irtg1792.hu-berlin.de](http://irtg1792.hu-berlin.de).

- 001 "Data Driven Value-at-Risk Forecasting using a SVR-GARCH-KDE Hybrid" by Marius Lux, Wolfgang Karl Härdle and Stefan Lessmann, January 2018.
- 002 "Nonparametric Variable Selection and Its Application to Additive Models" by Zheng-Hui Feng, Lu Lin, Ruo-Qing Zhu and Li-Xing Zhu, January 2018.
- 003 "Systemic Risk in Global Volatility Spillover Networks: Evidence from Option-implied Volatility Indices " by Zihui Yang and Yinggang Zhou, January 2018.
- 004 "Pricing Cryptocurrency options: the case of CRIX and Bitcoin" by Cathy YH Chen, Wolfgang Karl Härdle, Ai Jun Hou and Weining Wang, January 2018.
- 005 "Testing for bubbles in cryptocurrencies with time-varying volatility" by Christian M. Hafner, January 2018.
- 006 "A Note on Cryptocurrencies and Currency Competition" by Anna Almosova, January 2018.
- 007 "Knowing me, knowing you: inventor mobility and the formation of technology-oriented alliances" by Stefan Wagner and Martin C. Goossen, February 2018.
- 008 "A Monetary Model of Blockchain" by Anna Almosova, February 2018.
- 009 "Deregulated day-ahead electricity markets in Southeast Europe: Price forecasting and comparative structural analysis" by Antanina Hryshchuk, Stefan Lessmann, February 2018.
- 010 "How Sensitive are Tail-related Risk Measures in a Contamination Neighbourhood?" by Wolfgang Karl Härdle, Chengxiu Ling, February 2018.
- 011 "How to Measure a Performance of a Collaborative Research Centre" by Alona Zharova, Janine Tellingner-Rice, Wolfgang Karl Härdle, February 2018.
- 012 "Targeting customers for profit: An ensemble learning framework to support marketing decision making" by Stefan Lessmann, Kristof Coussement, Koen W. De Bock, Johannes Haupt, February 2018.
- 013 "Improving Crime Count Forecasts Using Twitter and Taxi Data" by Lara Vomfell, Wolfgang Karl Härdle, Stefan Lessmann, February 2018.
- 014 "Price Discovery on Bitcoin Markets" by Paolo Pagnottoni, Dirk G. Baur, Thomas Dimpfl, March 2018.
- 015 "Bitcoin is not the New Gold - A Comparison of Volatility, Correlation, and Portfolio Performance" by Tony Klein, Hien Pham Thu, Thomas Walther, March 2018.
- 016 "Time-varying Limit Order Book Networks" by Wolfgang Karl Härdle, Shi Chen, Chong Liang, Melanie Schienle, April 2018.
- 017 "Regularization Approach for Network Modeling of German EnergyMarket" by Shi Chen, Wolfgang Karl Härdle, Brenda López Cabrera, May 2018.

**IRTG 1792, Spandauer Straße 1, D-10178 Berlin**  
**<http://irtg1792.hu-berlin.de>**

This research was supported by the Deutsche  
Forschungsgemeinschaft through the IRTG 1792.

